NANO LETTERS

Letter

pubs.acs.org/NanoLett

Control of Single-Molecule Junction Conductance of Porphyrins via a Transition-Metal Center

Zhen-Fei Liu,*[,†] Sujun Wei,[‡] Hongsik Yoon,[§] Olgun Adak,[∥] Ingrid Ponce,[∥] Yivan Jiang,[‡] Woo-Dong Jang,[§] Luis M. Campos,*[,‡] Latha Venkataraman,*[,∥] and Jeffrey B. Neaton*[,†,⊥,#]

[†]Molecular Foundry and Materials Sciences Division, Lawrence Berkeley National Laboratory, Berkeley, California 94720, United States

[‡]Department of Chemistry, Columbia University, New York, New York 10027, United States

[§]Department of Chemistry, Yonsei University, 50 Yonsei-ro, Seodaemun-gu, Seoul 120-749, Republic of Korea

[∥]Department of Applied Physics and Applied Mathematics, Columbia University, New York, New York 10027, United States

[⊥]Department of Physics, University of California, Berkeley, California 94720, United States

[#]Kavli Energy Nanosciences Institute at Berkeley, Berkeley, California 94720, United States

Supporting Information

ABSTRACT: Using scanning tunneling microscope break-junction experiments and a new first-principles approach to conductance calculations, we report and explain low-bias charge transport behavior of four types of metal−porphyrin−gold molecular junctions. A nonequilibrium Green's function approach based on self-energy corrected density functional theory and optimally tuned range-separated hybrid functionals is developed and used to understand experimental trends quantitatively. Importantly, due to the localized d states of the porphyrin molecules, hybrid functionals are essential for explaining measurements; standard semilocal functionals yield qualitatively incorrect results. Comparing directly with experiments, we show that the conductance can change by nearly a factor of 2 when different metal cations are used, counter to trends expected from gas-phase ionization energies which are relatively unchanged with the metal center. Our work explains the sensitivity of the porphyrin conductance with the metal center via a detailed and quantitative portrait of the interface electronic structure and provides a new framework for understanding transport quantitatively in complex junctions involving molecules with localized d states of relevance to light harvesting and energy conversion.

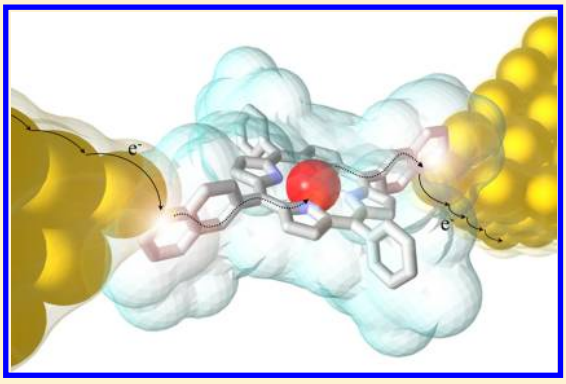

KEYWORDS: *Porphyrins and metalloporphyrins, single-molecule junction conductance, density functional theory, nonequilibrium Green's function, self-energy correction, range-separated hybrid functional*

Porphyrin-based molecules have attracted much attention in nanoscience and solar light harvesting applications[1−4] due to their highly conjugated backbones and strong absorption in the visible spectrum.[5] Crucial to further development of such systems for future applications is a nanoscale understanding of energy and charge transfer processes involving such molecules.[6−8] While spectroscopic studies can yield new insight via ensemble measurements, the development of break-junction techniques[9,10] has enabled reproducible measurement of the I−V characteristics,[11] conductance,[9] and thermopower[12] of junctions of individual molecular junctions,[13−16] especially at low bias.[17] Such studies provide a testbed for a fundamental understanding of the electronic structure at hybrid inorganic−organic interfaces, as they directly probe charge transfer at the molecular level. Prior experimental studies of porphyrin-based molecular junctions have focused on closed-shell systems, such as porphyrins with a Zn center,[16,18] but open-shell molecules[19] such as porphyrins with a Fe center[20−22] or a Cr center[23] can introduce additional unprecedented physical phenomena and functionality,[24−26] and more generally, trends in charge transport in such molecules with metal center have yet to be probed and elucidated.

In this work, we synthesize a series of both open- and closed-shell porphyrin-based molecules with different metal centers and measure their conductance in single-molecule junctions using the scanning tunneling microscope based break-junction (STM-BJ) technique. To understand the STM-BJ results, we develop and apply a new quantitative ab initio approach to compute conductance through these junctions. Our theoretical approach is based on self-energy corrected density functional theory (DFT), applied within the nonequilibrium Green's

Received: July 3, 2014
Revised: August 7, 2014

   dx.doi.org/10.1021/nl5025062 | *Nano Lett.* XXXX, XXX, XXX−XXX

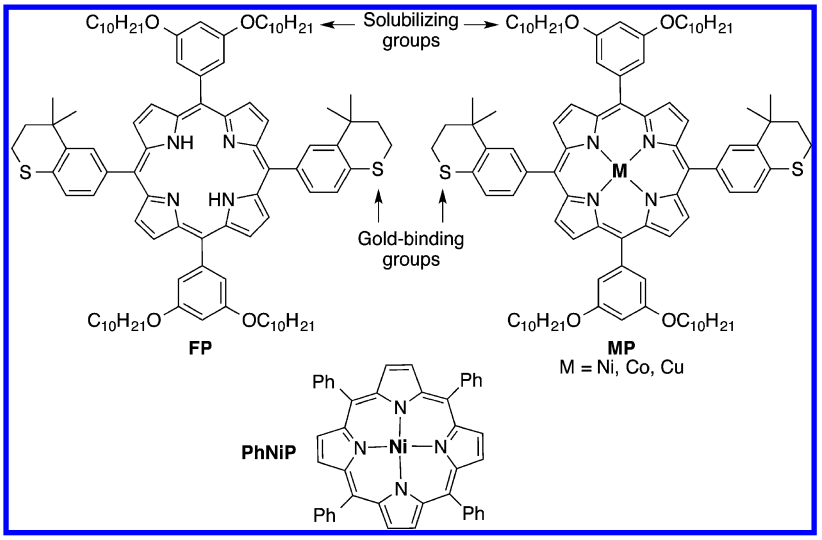

Figure 1. Chemical structures of FP and MP (M = Ni, Cu, Co) with locked alkyl sulfide linkers whose low-bias conductances are measured in break-junction experiments. To reduce computational cost, we replace the long alkyl group ($-C_{10}H_{21}$) with a methyl group ($-CH_3$). Also shown is the PhNiP used to validate the OT-RSH functional (see the Supporting Information). Its IP is known from experiment.[29]

function (NEGF) framework. Importantly, our approach is based on hybrid functionals to ensure the correct orbital ordering of the porphyrins, which can feature localized d states prominently. Our computational framework explains experiments quantitatively and lays the foundation for future transport studies for complex molecular systems, particularly those featuring localized d states prominently, and spin-related phenomena on surfaces.

The fundamental understanding of charge transport through metalloporphyrin building blocks in single-molecule junctions[9] has led to the discovery of several interesting phenomena, such as strong image-charge effects[16] and a low attenuation factor[13] in oligoporphyrins. Given the sensitivity of porphyrin structure on their single-molecule conductance properties, we investigate the role of metal ion coordination within the pyrrolic core to establish ion selectivity and metal ion identification through differences single-molecule conductance. The modularity of the porphyrins not only arises from ease of functionalization, but also from the variable metal ions that can be coordinated within the core. Herein, the soluble free porphyrin (FP) and metalloporphyrins shown in Figure 1 are synthesized, containing soluble groups along the methyne positions in one axis and thiochroman-based gold-binding groups along the other axis.[27] The metal ions are selected to compare both open-shell and closed-shell systems. For example, cobalt- and copper-containing porphyrins (CoP and CuP, respectively) are open-shell species,[28] as opposed to the nickel and zinc porphyrins (NiP and ZnP, respectively), but their charge transport properties on contact with electrodes are unknown.

Theoretical studies of charge transport in molecular junctions primarily make use of either scattering theory[30,31] or NEGF theory.[32] In the linear response regime, these two approaches are equivalent.[32,33] Ab initio calculations of transport in molecular junctions[34] with either approach most commonly employ DFT[35−37] in standard approximations, as DFT strikes a balance among computational cost, chemical specificity, and accuracy for ground-state properties. However, with popular local or semilocal functionals, such as the local density approximation (LDA)[38] and generalized gradient approximations (GGAs),[39] the alignment between frontier orbital energies and the junction Fermi level is significantly underestimated,[40,41] leading to an overestimated conductance, usually by an order of magnitude or more.[42,43] Equivalently, the poles in Kohn−Sham (KS) Green's functions for the junction differ significantly from the exact one-particle Green's functions,[44] limiting the utility of DFT-based transport approaches. A promising alternative is to combine transport frameworks with many-body perturbation theory (MBPT) within the GW approximation,[42,45] although often at great computational expense, limiting the complexity of junctions accessible to this approach. An accurate but more approximate and computationally less expensive GW method is the DFT+Σ method, which can correct for junction level alignment and has been successful for explaining many recent experiments.[42,46,47] In DFT+Σ,[42,46] a GW-based self-energy correction is made to the eigenvalues of the molecular subspace of the combined electrode−molecule−electrode system, taking into account (i) the inaccuracy of gas-phase frontier orbital energies from LDA or GGAs and (ii) nonlocal static correlations associated with surface polarization.[40] DFT+Σ works well for a broad array of molecules with different linkers, such as amines,[42,46] pyridines,[48,47] and phosphines,[17] resulting in quantitative agreement with experiment,[42,46] greatly improving over GGA results. However, for systems with highly localized d states[49] such as the metal porphyrins, complications can arise. Prior work has shown that, using local or semilocal functionals, the calculated dominating conducting orbital may not be the true frontier orbital because of significant self-interaction errors,[50] particularly for metal porphyrins; introducing a fraction of exact exchange[51] via hybrid functionals led to ordering in agreement with photoemission spectroscopy.[52−54] In this work, we extend the DFT+Σ scheme under the NEGF framework to treat junctions with localized d states using a new class of hybrid functionals, the optimal-tuned range-separated hybrid functionals (OT-RSHs),[55] not only because they possess a fraction of exact exchange but also because they lead to accurate ionization potentials by construction.[56,57] We demonstrate it can explain quantitatively the trends in conductance of porphyrin-based molecular junctions.

The synthesis of the porphyrins was carried out via a standard procedure,[3] and the thiochroman gold-binding groups were chosen for their ability to form stable junctions with gold electrodes.[27] Having synthesized FP, the different metal ions

dx.doi.org/10.1021/nl5025062 | Nano Lett. XXXX, XXX, XXX−XXX

were incorporated by adding select metal(II) salts in solution by refluxing. We show the UV−vis absorption spectra of FP and metal porphyrins in the Supporting Information, which shows clear differences arising from the S0−S1 transition (Q band), whereas the dominant higher energy S0−S2 transition remains relatively unchanged (B band). Such data provide clear evidence that the core of FP was successfully metalated with various ions.

We carried out break-junction measurements of low-bias conductance for four different porphyrin-based molecules. The conductance measurements were done using the scanning tunneling microscope break junction (STM-BJ) technique under ambient conditions.[10] Molecular solutions prepared with 1,2,4-trichlorobenzene were deposited onto gold-on-mica substrate. Thousands of molecular junctions were obtained by repeatedly pulling the gold tip out of the substrate, and their conductance was measured at a 400 mV bias voltage. The conductance traces were compiled into logarithmically binned one-dimensional histograms, which yielded the most probable conductance peak value for each molecule (Figure 2a).

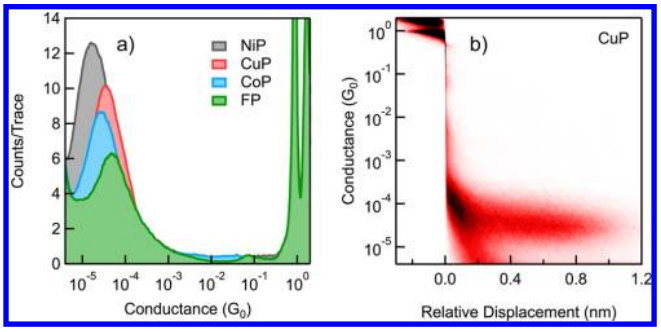

Figure 2. (a) Logarithmically binned one-dimensional conductance histogram of the porphyrin systems studied in this work. (b) Logarithmically binned two-dimensional conductance histogram of CuP.

Additionally, two-dimensional histograms were obtained in order to confirm the formation of stable single-molecule junctions (Figure 2b shows the result for CuP). These show a displacement step length around 9 Å that is proportional to the length of the molecule across the conductance path. All four molecules form junctions whose conductance values differ by about a factor of 2.

To understand the measured conductance and trends, we turn to ab initio DFT-based transport calculations. For our calculations, we constructed model junction geometries using the fact that locked alkyl sulfide linkers binds selectively to undercoordinated Au atoms via the lone pair of the S atoms[27] and a donor−acceptor mechanism, similar to the case for the amines.[58] We thus used an adatom binding motif (see Figure 3) in modeling the junction geometry, analogous to those successfully used in past studies on amine−Au junctions.[42] We replaced the long alkyl group ($-C_{10}H_{21}$) with a methyl group ($-CH_3$). This simplifies our calculation, allowing the molecule to fit into a junction with 64 (8 × 8) gold atoms per atomic layer, while having negligible impact on electronic and transport properties. By direct calculation using the same functional, we find that removing the alkyl group leads to nearly the same gas-phase ionization potential (IP).

Our junction geometries were relaxed using spin-unrestricted DFT with the Perdew−Burke−Ernzerhof (PBE)[39] functional as implemented in SIESTA.[59] Pseudopotentials and basis sets for gold and other atoms were adapted from previous work.[42,46,47] We used four atomic layers of gold on each side in the relaxation of the junction, with the outer two layers on each side held fixed in the bulk geometry, while their coordinates along the transport axis were allowed to relax (see the Supporting Information). Periodic boundary conditions with Gamma k-point sampling were used in all relaxations. Atomic positions were optimized until forces were smaller than 0.04 eV/Å. Figure 3 shows the geometry of the system in our transmission calculations, which includes a molecule with seven gold atomic layers on each side. The optimized Au−S bond length was about 2.7 Å, and the calculated angle between the Au−S bonds and the neighboring aromatic rings was about 140°.[60] We found that, in the gas phase, the ground states of both NiP and FP are closed shell and those of CuP and CoP are low-spin open shell, consistent with experiment.[28] With geometries optimized as above, we carried out transport calculations using TranSIESTA[61] with the same functional, pseudopotentials, and basis set. Seven layers of gold were required on each side of the junction to converge our calculations of the transmission, with the last three layers on each side as the left/right electrode. A 3 × 3 $k_{\|}$-mesh (4 × 4 for NiP and CuP) was used. To converge the steady-state charge density, 36 energy grids were used in the energy contour integration.[61] The transmission was computed in the direction perpendicular to the gold atomic layers, and periodic boundary conditions were used in the other two transverse directions.

Using the method described above, we could compute transmission functions $T(E)$ for all four molecules using PBE. However, we will show below that this leads to qualitatively incorrect results for transition-metal porphyrins, and hybrid

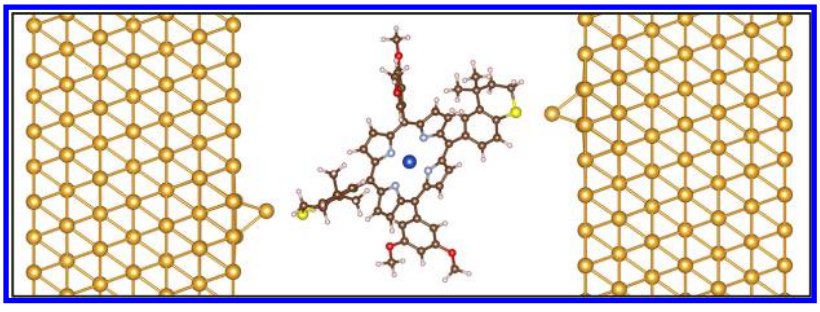

Figure 3. CuP molecular junction geometry used in this work. Periodic boundary conditions are used perpendicular to the current flow (left to right in this figure). In our calculations, seven layers of gold are required on each side to converge the results, with the last three layers on each side (fixed at their bulk geometry) as the left/right electrodes. For other systems studied in this work, Cu is replaced by Ni (NiP), Co (CoP), or two hydrogens (FP).

dx.doi.org/10.1021/nl5025062 | Nano Lett. XXXX, XXX, XXX−XXX

functionals, which mix in a fraction of exact exchange, are necessary. The DFT-PBE transmission function, $T(E)$, for the NiP junction is shown in Figure 4. The computed value of

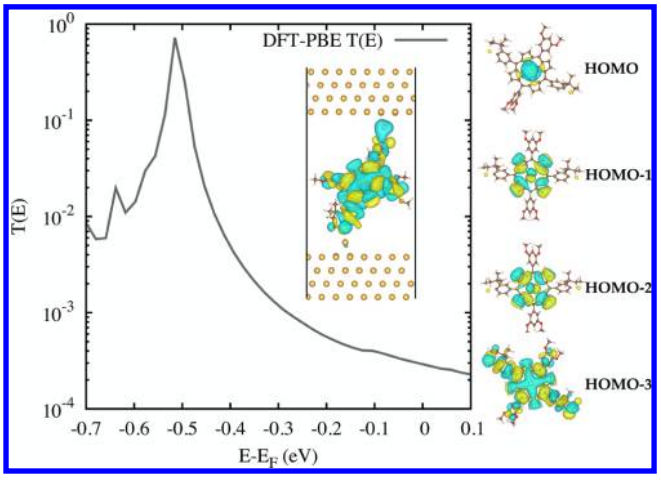

Figure 4. DFT-PBE transmission function, $T(E)$, for the NiP–Au junction. Inset: eigenchannel at $E = E_F - 0.51$ eV (the resonance energy). This eigenchannel dominates conductance at E_F. On the right-hand side are shown NiP gas-phase Kohn–Sham orbitals from PBE. From top to bottom are the HOMO, HOMO-1, HOMO-2, and HOMO-3.

$T(E_F)$ and therefore the conductance is overestimated (as expected[43]): we computed 2.9×10^{-4} G_0, where $G_0 = 2e^2/h$. For comparison, the average experimental low-bias conductance is 1.9×10^{-5} G_0 for NiP. The overestimated PBE conductance is a consequence of the frontier orbital resonance energy being underestimated.[40] In addition to the conductance, the inset of Figure 4 shows that the dominant conducting orbital for the junction is the molecular HOMO-3, as determined from an eigenchannel analysis using the Inelastica package.[62] However, given that this assignment is based on PBE, there are reasons to question its validity. PBE (and all local and semilocal functionals) inadequately treats localized d states due to self-interaction errors.[50] This has been demonstrated specifically for metal–porphyrin molecules, where hybrid functionals are shown to lead to qualitatively different orbital ordering.[53,54]

To explore the consequences of a hybrid functional on metal–porphyrin electronic structure, we calculated gas-phase orbitals using both PBE and OT-RSH functionals.[55] We used the optimized PBE geometry using the 6-311G(d,p) basis set implemented in QChem.[63] Spin-unrestricted calculations were performed, and for all systems considered here, the predicted ground state of the molecules was a low-spin configuration, consistent with experiment.[28] The OT-RSH functional[55] has two parameters α and γ, which were tuned to satisfy the exact conditions of DFT. We fixed α, which determines the fraction of short-range exact exchange, to 0.2, which is a reasonable choice on the basis of previous work[56,57] and yields excellent results. We optimized γ, the range separation parameter, following the strategy in ref 56 for the isolated molecules. We found that $\alpha = 0.2$ and $\gamma = 0.1$ perform well for all systems considered in this work. Details of our calculations using the OT-RSH functional can be found in the Supporting Information. We then computed the projection $\langle\psi(\text{PBE})|\psi(\text{OT-RSH})\rangle$ to determine any differences in the relative orbital orderings from the two functionals. We see that the orbital ordering does indeed differ significantly: the PBE HOMO-3 corresponds to the OT-RSH HOMO (their inner product is almost unity). In other words, if we were to calculate $T(E)$ directly using OT-RSH, presently challenging due to the high computational cost of using a hybrid functional for extended systems, the dominating conducting orbital would be identified as the HOMO, rather than the HOMO-3.

The above NiP junction example demonstrates the necessity of using a hybrid, such as the OT-RSH functional, to correct PBE orbital ordering in metal–porphyrin systems. This issue is absent in the FP, as there are no localized d states. Indeed, for FP, we see the dominating conducting orbital from both the PBE and the OT-RSH calculations is the HOMO.

Applying the above procedure for all four systems, we report DFT+Σ and PBE results for computed conductance values for all junctions in Table 1 and in Figure 5, comparing to experiment. DFT+Σ results improve significantly over those of PBE and agree quantitatively and trendwise with experiment. In general, DFT+Σ leads to a slightly lower low-bias conductance than experiment, and there are several possible explanations for this deviation. First, all experiments were done in solution, and our calculations neglected solvent effects. Second, there is uncertainty in the junction geometry: we are comparing a single geometry with an adatom binding motif with the peak conductance value of a histogram; changes in binding geometry can alter conductances, as is event from the width of these distributions. Moreover, to reduce computational cost, we eliminated the long alkyl group ($-C_{10}H_{21}$) and replaced it with a methyl group ($-CH_3$). Although this has minimal effect on the molecular IP, it may affect the geometry and coverage of the molecule in the junction, which can also affect conductance.[64]

Table 1. Comparison of Conductances from Break-Junction Experiments, DFT-PBE Calculations, and DFT+Σ Calculations using OT-RSH Functional[a]

	FP	CuP	CoP	NiP
exptl conductance ($\times 10^{-5} G_0$)	4.6	3.6	2.5	1.9
DFT-PBE conductance ($\times 10^{-5} G_0$)	127	72 (44 + 28)	38 (19 + 19)	29
DFT+Σ conductance ($\times 10^{-5} G_0$)	1.3	0.98 (0.54 + 0.44)	0.51 (0.25 + 0.26)	0.49
DFT+Σ $E_F - \varepsilon_{HOMO}$ (eV)	1.51	1.50/1.63	1.68/1.67	1.77
OT-RSH gas phase IP (eV)	5.77	5.85	5.89	5.88
level broadening (eV)	0.009	0.008/0.008	0.008/0.008	0.008

[a]We compare trends in conductance to trends in gas-phase IP, self-energy corrected level alignment ($E_F - \varepsilon_{HOMO}$ using DFT+Σ), and level broadening (fitted from a simple Lorentzian form). For spin-polarized cases such as CuP and CoP, contributions to the conductance from two spin components are given in parentheses with the format (majority spin + minority spin), and for other quantities, two spin components are given in parentheses as majority spin/minority spin.

dx.doi.org/10.1021/nl5025062 | Nano Lett. XXXX, XXX, XXX–XXX

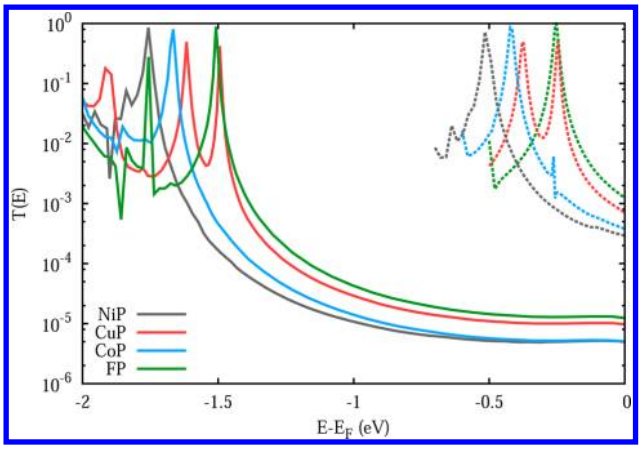

Figure 5. Transmission functions $T(E)$ for four different metal–porphyrin junctions, calculated from DFT-PBE (dashed lines) and DFT+Σ (solid lines).

Third, our IP, which features prominently in our self-energy calculations, may suffer from slight inaccuracies. There are, as yet, no experimental IP values available for comparison.

We also mention a few additional sources of error. First, using OT-RSH to correct the PBE level ordering, we assume the difference between the OT-RSH HOMO energy and PBE conducting orbital energy in the gas phase is same as the difference in the junction. This approximation can suffer from errors in PBE junction level alignment and interface dipoles.[65] Finally, we mention possible errors in estimating contributions to the junction self-energy as a static image charge interaction. This has been extensively discussed in ref 40, and we refer the readers to that work.

From Figure 5 and Table 1, we see that the conductance trend follows that of the self-energy corrected level alignment (distance between the main peaks in $T(E)$ and Fermi level; also see the $E_F - \varepsilon_{HOMO}$ line in Table 1). The only exception is CuP, whose majority spin HOMO is slightly higher than the FP HOMO (although the CuP conductance is smaller than that of FP). This is because CuP has non-negligible spin splitting at the HOMO level and each spin component couples to the lead individually, making the effective coupling smaller than that for the FP HOMO. The junction level alignment consists of three contributions, one from the gas-phase IP, one from the interface dipole induced upon binding, and one from surface polarization. The gas-phase IP is also given in Table 1, and we see that it differs among the four molecules by only about 0.1 eV, while the level alignment difference is about 0.26 eV. In particular, FP has the lowest gas-phase IP and therefore has the deepest HOMO resonance energy. For the other three molecules, the IPs are similar, and the difference in level alignment is due to differences in interface dipole. We also note in passing that, from Table S1 in the Supporting Information, the self-energy corrections for all systems are very similar, and thus at the PBE level, the trend in conductance for this series of molecules is captured, although the actual values are significantly larger—by 2 orders of magnitude in some cases—than experiment. This can be attributed in part to the good accuracy of the PBE interface dipole.[65] The differences in conductance among systems can thus be understood as related to subtle differences in electronegativity of different metals in the center.

For the two open-shell systems (CuP and CoP), conductances for both spin components are similar, as the HOMO resonance of both spin components are far away from E_F and spin splitting is small. In the Supporting Information, we show the spin-dependent $T(E)$ for the two open-shell systems, CuP and CoP, respectively, calculated both from PBE and DFT +Σ. For molecular junctions to exhibit significant magneto-resistance with nonmagnetic leads, one needs an open-shell molecule and either large spin splitting between the two spin channels and/or HOMO (or LUMO) resonances of both spin components near the junction Fermi level. This is an interesting area of future study.

In this work, our calculations yielded quantitative agreement with experiments, and we found that by changing the central metal atom, the conductance could be altered by up to a factor of 2. We emphasize that, for such complex systems involving transition-metal atoms, transmission calculations using local or semilocal functionals could be qualitatively incorrect, and hybrid functionals such as OT-RSH containing a fraction of exact exchange are necessary to preserve orbital ordering and accurate self-energy corrections.

■ ASSOCIATED CONTENT

Supporting Information

Text, a table, and figures giving, for the theoretical study, detailed information on optimization of the geometry, self-energy corrections with hybrid functionals, Landauer formula using DFT+Σ, spin-dependent $T(E)$ for CoP and CuP, and the block-zero form of coupling matrices and, for the experimental study, materials and general methods, UV–vis spectra, synthetic procedures, and NMR spectra. This material is available free of charge via the Internet at http://pubs.acs.org.

■ AUTHOR INFORMATION

Corresponding Authors

*E-mail for Z.-F.L.: zfliu@lbl.gov.
*E-mail for L.M.C.: lcampos@columbia.edu.
*E-mail for L.V.: lv2117@columbia.edu.
*E-mail for J.B.N.: jbneaton@lbl.gov.

Notes

The authors declare no competing financial interest.

■ ACKNOWLEDGMENTS

Z.-F.L. thanks Michele Kotiuga and Hector Vazquez for discussion of the use of SIESTA and TranSIESTA packages and Sivan Refaely-Abramson and Shira Weissman for discussion of the OT-RSH functional. The computational part of this work was supported by the U.S. Department of Energy, Office of Basic Energy Sciences, Materials Sciences and Engineering Division, under Contract No. DE-AC02-05CH11231. A portion of this work was also supported by the Molecular Foundry through the U.S. Department of Energy, Office of Basic Energy Sciences, under the same contract number. A portion of the computation work was done using NERSC resources. The experimental portions of this work were supported by NSF Grant DMR-1206202 (L.V., S.W., and L.M.C.). I.P. is grateful to Fondecyt Project 3140104.

■ REFERENCES

(1) Hasobe, T. *J. Phys. Chem. Lett.* **2013**, *4*, 1771.
(2) Yoon, H.; Lim, J. M.; Gee, H.-C.; Lee, C.-H.; Jeong, Y.-H.; Kim, D.; Jang, W.-D. *J. Am. Chem. Soc.* **2014**, *136*, 1672.
(3) Jeong, Y.-H.; Son, M.; Yoon, H.; Kim, P.; Lee, D.-H.; Kim, D.; Jang, W.-D. *Angew. Chem.* **2014**, *126*, 7045–7048.

(4) Kim, J.-H.; Jeong, Y.-H.; Yoon, H.-J.; Tran, H.; Campos, L.; Jang, W.-D. *Chem. Commun.* **2014**, DOI: 10.1039/C4CC05261G.
(5) *The Porphyrin Handbook*; Kadish, K., Guilard, R., Smith, K. M., Eds.; Academic Press: San Diego, CA, 2002; Phthalocyanines: Spectroscopic and Electrochemical Characterization, Vol. *16*.
(6) Hagfeldt, A.; Boschloo, G.; Sun, L.; Kloo, L.; Pettersson, H. *Chem. Rev.* **2010**, *110*, 6595−6663.
(7) Scharber, M. C.; Mühlbacher, D.; Koppe, M.; Denk, P.; Waldauf, C.; Heeger, A. J.; Brabec, C. J. *Adv. Mater.* **2006**, *18*, 789−794.
(8) Jiang, J.-X.; Wang, C.; Laybourn, A.; Hasell, T.; Clowes, R.; Khimyak, Y. Z.; Xiao, J.; Higgins, S. J.; Adams, D. J.; Cooper, A. I. *Angew. Chem., Int. Ed.* **2011**, *50*, 1072.
(9) Xu, B. Q.; Tao, N. J. *Science* **2003**, *301*, 1221−1223.
(10) Venkataraman, L.; Klare, J. E.; Nuckolls, C.; Hybertsen, M. S.; Steigerwald, M. L. *Nature* **2006**, *442*, 904−907.
(11) Widawsky, J. R.; Kamenetska, M.; Klare, J.; Nuckolls, C.; Steigerwald, M. L.; Hybertsen, M. S.; Venkataraman, L. *Nanotechnology* **2009**, *20*, 434009.
(12) Reddy, P.; Jang, S. Y.; Segalman, R. A.; Majumdar, A. *Science* **2007**, *315*, 1568.
(13) Sedghi, G.; Garcia-Suarez, V. M.; Esdaile, L. J.; Anderson, H. L.; Lambert, C. J.; Martin, S.; Bethell, D.; Higgins, S. J.; Elliott, M.; Bennett, N.; Macdonald, J. E.; Nichols, R. J. *Nat. Nanotechnol.* **2011**, *6*, 517.
(14) Li, Z.; Borguet, E. *J. Am. Chem. Soc.* **2012**, *134*, 63.
(15) Li, Z.; Smeu, M.; Ratner, M. A.; Borguet, E. *J. Phys. Chem. C* **2013**, *117*, 14890.
(16) Perrin, M. L.; Verzijl, C. J. O.; Martin, C. A.; Shaikh, A. J.; Eelkema, R.; van Esch, J. H.; van Ruitenbeek, J. M.; Thijssen, J. M.; van der Zant, H. S. J.; Dulić, D. *Nat. Nanotechnol.* **2013**, *8*, 282−287.
(17) Widawsky, J. R.; Darancet, P.; Neaton, J. B.; Venkataraman, L. *Nano Lett.* **2012**, *12*, 354.
(18) Ribeiro, F. J.; Lu, W.; Bernholc, J. *ACS Nano* **2008**, *2*, 1517.
(19) Park, J.; Pasupathy, A. N.; Goldsmith, J. I.; Chang, C.; Yaish, Y.; Petta, J. R.; Rinkoski, M.; Sethna, J. P.; na, H. D. A.; McEuen, P. L.; Ralph, D. C. *Nature* **2002**, 722−725.
(20) Chen, Y.; Prociuk, A.; Perrine, T.; Dunietz, B. D. *Phys. Rev. B* **2006**, *74*, 245320.
(21) Kondo, H.; Kino, H.; Nara, J.; Ohno, T. *Appl. Surf. Sci.* **2008**, *254*, 7985−7988.
(22) Salazar-Salinas, K.; Jauregui, L. A.; Kubli-Garfias, C.; Seminario, J. M. *J. Chem. Phys.* **2009**, *130*, 105101.
(23) Cho, W. J.; Cho, Y.; Min, S. K.; Kim, W. Y.; Kim, K. S. *J. Am. Chem. Soc.* **2011**, *133*, 9364−9369.
(24) Zhao, A.; Li, Q.; Chen, L.; Xiang, H.; Wang, W.; Pan, S.; Wang, B.; Xiao, X.; Yang, J.; Hou, J. G.; Zhu, Q. *Science* **2005**, *309*, 1542−1544.
(25) Schmaus, S.; Bagrets, A.; Nahas, Y.; Yamada, T. K.; Bork, A.; Bowen, M.; Beaurepaire, E.; Evers, F.; Wulfhekel, W. *Nat. Nanotechnol.* **2011**, *6*, 185−189.
(26) Gorjizadeh, N.; Quek, S. Y. *Nanotechnology* **2013**, *24*, 415201.
(27) Park, Y. S.; Widawsky, J. R.; Kamenetska, M.; Steigerwald, M. L.; Hybertsen, M. S.; Nuckolls, C.; Venkataraman, L. *J. Am. Chem. Soc.* **2009**, *131*, 10820−10821.
(28) *The porphyrin handbook*; Kadish, K. M., Smith, K. M., Guilard, R., Eds.; Academic Press: San Diego, CA, 2000; Vol. *3*.
(29) Khandelwal, S. C.; Roebber, J. L. *Chem. Phys. Lett.* **1975**, *34*, 355−359.
(30) Landauer, R. *IBM J. Res. Dev.* **1957**, *1*, 223−231.
(31) Fisher, D. S.; Lee, P. A. *Phys. Rev. B* **1981**, *23*, 6851−6854.
(32) Meir, Y.; Wingreen, N. S. *Phys. Rev. Lett.* **1992**, *68*, 2512−2515.
(33) Haug, H. J. W.; Jauho, A.-P. *Quantum Kinetics in Transport and Optics of Semiconductors*, 2nd ed.; Springer: Berlin, 2007.
(34) Di Ventra, M.; Pantelides, S. T.; Lang, N. D. *Phys. Rev. Lett.* **2000**, *84*, 979−982.
(35) Dreizler, R. M.; Gross, E. K. U. *Density functional theory: An approach to the quantum many-body problem*; Springer-Verlag: Berlin, 1990.
(36) Burke, K. *J. Chem. Phys.* **2012**, *136*, 150901.
(37) Becke, A. D. *J. Chem. Phys.* **2014**, *140*, 18A301.
(38) Kohn, W.; Sham, L. J. *Phys. Rev.* **1965**, *140*, A1133−A1138.
(39) Perdew, J. P.; Burke, K.; Ernzerhof, M. *Phys. Rev. Lett.* **1996**, *77*, 3865−3868; **1997**, *78*, 1396 (E).
(40) Neaton, J. B.; Hybertsen, M. S.; Louie, S. G. *Phys. Rev. Lett.* **2006**, *97*, 216405.
(41) Dell'Angela, M.; Kladnik, G.; Cossaro, A.; Verdini, A.; Kamenetska, M.; Tamblyn, I.; Quek, S. Y.; Neaton, J. B.; Cvetko, D.; Morgante, A.; Venkataraman, L. *Nano Lett.* **2010**, *10*, 2470−2474.
(42) Quek, S. Y.; Venkataraman, L.; Choi, H. J.; Louie, S. G.; Hybertsen, M. S.; Neaton, J. B. *Nano Lett.* **2007**, *7*, 3477−3482.
(43) Lindsay, S. M.; Ratner, M. A. *Adv. Mater.* **2007**, *19*, 23.
(44) Koentopp, M.; Chang, C.; Burke, K.; Car, R. *J. Phys.: Condens. Matter* **2008**, *20*, 083203.
(45) Thygesen, K. S.; Rubio, A. *Phys. Rev. B* **2008**, *77*, 115333.
(46) Quek, S. Y.; Choi, H. J.; Louie, S. G.; Neaton, J. B. *Nano Lett.* **2009**, *9*, 3949−3953.
(47) Darancet, P.; Widawsky, J. R.; Choi, H. J.; Venkataraman, L.; Neaton, J. B. *Nano Lett.* **2012**, *12*, 6250−6254.
(48) Quek, S. Y.; Kamenetska, M.; Steigerwald, M. L.; Choi, H. J.; Louie, S. G.; Hybertsen, M. S.; Neaton, J. B.; Venkataraman, L. *Nat. Nanotechnol.* **2009**, *4*, 230−234.
(49) Svane, A.; Gunnarsson, O. *Phys. Rev. Lett.* **1990**, *65*, 1148−1151.
(50) Perdew, J. P.; Zunger, A. *Phys. Rev. B* **1981**, *23*, 5048−5079.
(51) Becke, A. D. *J. Chem. Phys.* **1993**, *98*, 5648−5652.
(52) Liao, M.-S.; Scheiner, S. *J. Chem. Phys.* **2002**, *117*, 205−219.
(53) Marom, N.; Hod, O.; Scuseria, G. E.; Kronik, L. *J. Chem. Phys.* **2008**, *128*, 164107.
(54) Marom, N.; Kronik, L. *Appl. Phys. A: Mater. Sci. Process.* **2009**, *95*, 159−163.
(55) Stein, T.; Eisenberg, H.; Kronik, L.; Baer, R. *Phys. Rev. Lett.* **2010**, *105*, 266802.
(56) Refaely-Abramson, S.; Sharifzadeh, S.; Govind, N.; Autschbach, J.; Neaton, J. B.; Baer, R.; Kronik, L. *Phys. Rev. Lett.* **2012**, *109*, 226405.
(57) Refaely-Abramson, S.; Sharifzadeh, S.; Jain, M.; Baer, R.; Neaton, J. B.; Kronik, L. *Phys. Rev. B* **2013**, *88*, 081204.
(58) Venkataraman, L.; Klare, J. E.; Tam, I. W.; Nuckolls, C.; Hybertsen, M. S.; Steigerwald, M. L. *Nano Lett.* **2006**, *6*, 458−462.
(59) Soler, J. M.; Artacho, E.; Gale, J. D.; Garca, A.; Junquera, J.; Ordejón, P.; Sánchez-Portal, D. *J. Phys.: Condens. Matter* **2002**, *14*, 2745.
(60) The metal-nitrogen bond lengths are 1.98, 1.98, and 2.05 Å for NiPc, CoPc, and CuPc, respectively.
(61) Brandbyge, M.; Mozos, J.-L.; Ordejón, P.; Taylor, J.; Stokbro, K. *Phys. Rev. B* **2002**, *65*, 165401.
(62) Paulsson, M.; Brandbyge, M. *Phys. Rev. B* **2007**, *76*, 115117.
(63) Shao, Y.; et al. *Phys. Chem. Chem. Phys.* **2006**, *8*, 3172.
(64) Fatemi, V.; Kamenetska, M.; Neaton, J. B.; Venkataraman, L. *Nano Lett.* **2011**, *11*, 1988.
(65) Biller, A.; Tamblyn, I.; Neaton, J. B.; Kronik, L. *J. Chem. Phys.* **2011**, *135*, 164706.